J|A|C|S
ARTICLES
Published on Web 04/02/2004

Molecular Interactions in One-Dimensional Organic Nanostructures

Thuc-Quyen Nguyen,*,† Richard Martel,*,‡,§ Phaedon Avouris,‡ Mark L. Bushey,† Louis Brus,† and Colin Nuckolls*,†

Contribution from the Department of Chemistry, Columbia University, New York, New York 10027, and IBM Watson Research Center, Yorktown Heights, New York

Received December 9, 2003; E-mail: tqn@chem.columbia.edu; r.martel@umontreal.ca; cn37@columbia.edu

Abstract: Intermolecular interactions involving $\pi-\pi$ interaction and hydrogen bonding are used to create one-dimensional molecular nanostructures of hexasubstituted aromatics. Site-selective steady state fluorescence, time-resolved fluorescence, scanning electron microscopy, and atomic force microscopy measurements detail the intermolecular interactions that drive the aromatic molecules to self-assemble in solution to form well-ordered columnar stacks. These nanostructures, formed in solution, vary in their number, size, and structure depending on the solvent used. In addition, our results indicate that the substituents/side groups and the proper choice of the solvent can be used to tune the intermolecular interactions. The 1D stacks and their aggregates can be easily transferred by solution casting, thus allowing a simple preparation of molecular nanostructures on different surfaces.

I. Introduction

Detailed below is the self-assembly characteristics of hydrogen-bond enforced, crowded aromatics into one-dimensional π-stacks in solution and on substrates. The assembly can be monitored with optical spectroscopy due to ground and excited states being electronically delocalized upon assembly. These stacks maintain their electronic structure when transferred to graphite and silicon substrates and can be visualized with scanning electron microscopy (SEM) and atomic force microscopy (AFM). In general, π-stacking is useful because it provides a route to plastic materials that could have utility in electronics application. Functionalization of disk-shaped aromatic molecules with hydrocarbon chains[1] has been shown to be a useful method to influence π-stacking and to create one-dimensional electronic materials.[2,3] One aspect of these π-stacked materials that remains unexplored is how their optical and electronic properties vary as the size of the stack is decreased to near molecular length-scales. To begin to address this problem, robust assembly motifs for aromatic molecules are needed that go beyond traditional π-stacking to allow isolated nanostructures to be formed and probed. However, it is not only important to master the intermolecular assembly but also to understand how to form and interface these assemblies with useful substrates.[4−6] The study below utilizes the hexasubstituted aromatic molecules shown in Figure 1 to help understand the interplay between solution-phase assembly and the morphology in thin films.

Compounds **1** and **2** belong to a class of hexasubstituted aromatic compounds that assemble to have an internal π-stacked core that is surrounded by an outer insulating sheath of alkyl groups.[4,7] Both **1** and **2** were recently shown to form discotic liquid crystalline phases in bulk and to assemble into isolated 1D nanostructures in monolayer films on graphite.[7c] In addition to the $\pi-\pi$ interactions that characterize the assembly in classical discotic liquid crystals,[1] each subunit here contains three hydrogen bonds[3,5,8] formed from the metadisposed amide groups. The steric congestion in the central core creates a directionality to the amide hydrogen bonds that enforces the stacking into a columnar structure. The size of the group that flanks the amides determines the degree that the amide twists

† Columbia University.
‡ IBM Watson Research Center.
§ Present address: Chemistry Department, Université de Montréal, Montréal, Canada.

(1) For leading references on discotic liquid crystals, see: (a) Destrade, C.; Foucher, P.; Gasparoux, H.; Nguyen, H. T.; Levelut, A. M.; Malthete, J. *Mol. Cryst. Liq. Cryst.* **1984**, *106*, 121−146. (b) Chandrasekhar, S.; Ranganath, G. S. *Rep. Prog. in Phys.* **1990**, *53*, 57−84. (c) Chandrasekhar, S.; Prasad, S. K. *Contemporary Phys.* **1999**, *40*, 237−245. (d) Chandrasekhar, S. *Handbook Liq. Cryst.* **1998**, *2B*, 749−780. (e) Guillon, D. *Struct. Bonding* (*Berlin*) **1999**, *95*, 41−82.

(2) In bulk, several columnar π-stacks have shown potential as one-dimensional electronic materials, see: (a) Boden, N.; Movaghar, B. *Handbook Liq. Cryst.* **1998**, *2B*, 781−798. (b) Boden, N.; Bushby, R. J.; Clements, J.; Movaghar, B. *J. Mater. Chem.* **1999**, *9*, 2081−2086. (c) van de Craats, A. M.; Stutzmann, N.; Bunk, O.; Nielsen, M. M.; Watson, M.; Mullen, K.; Chanzy, H. D.; Sirringhaus, H.; Friend, R. H. *Adv. Mater.* **2003**, *15*, 495−499. (d) Schmidt-Mende, L.; Fechtenkotter, A.; Mullen, K.; Moons, E.; Friend, R. H.; MacKenzie, J. D. *Science* **2001**, *293*, 1119−1122. (e) Percec, V.; Glodde, M.; Bera, T. K.; Miura, Y.; Shiyanovskaya, I.; Singer, K. D.; Balagurusamy, V. S. K.; Heiney, P. A.; Schnell, I.; Rapp, A.; Spiess, H. W.; Hudson, S. D.; Duan, H. *Nature* **2002**, *419*, 384−387.

(3) Gearba, R. I.; Lehmann, M.; Levin, J.; Ivanov, D. A.; Koch, M. H. J.; Barbera, J.; Debije, M. G.; Piris, J.; Geerts, Y. H. *Adv. Mater.* **2003**, *15*, 1614−1618.

(4) (a) Nguyen, T.-Q.; Bushey, M. L.; Brus, L. E.; Nuckolls, C. *J. Am. Chem. Soc.* **2002**, *124*, 15051−15054. (b) Tulevski, G. S.; Bushey, M. L.; Kosky, J. L.; Ruter, S. J. T.; Nuckolls, C. *Angew. Chem., Int. Ed.*, in press.

(5) van Gorp, J. J.; Vekemans, J. A. J. M.; Meijer, E. W. *J. Am. Chem. Soc.* **2002**, *124*, 14759−14769.

(6) Johnkheijm, P.; Hoeben, F. J. M.; Kleppinger, R.; van Herrikhuyzen, J.; Schenning, A. P. H. J.; Meijer, E. W. *J. Am. Chem. Soc.* **2003**, ASAP.

(7) (a) Bushey, M. L.; Hwang, A.; Stephens, P. W.; Nuckolls, C. *J. Am. Chem. Soc.* **2001**, *123*, 8157−8158. (b) Bushey, M. L.; Hwang, A.; Stephens, P. W.; Nuckolls, C. *Angew. Chem., Int. Ed.* **2002**, *41*, 2828−2831. (c) Bushey, M. L.; Nguyen, T.-Q.; Nuckolls, C. *J. Am. Chem. Soc.* **2003**, *125*, 8264−8269.

 10.1021/ja031600b CCC: $27.50

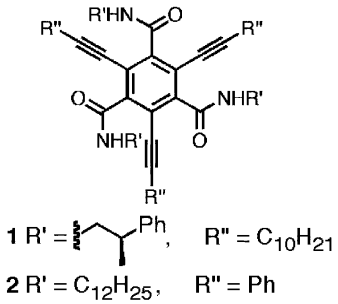

Figure 1. Chemical structures of compounds studied, **1** and **2**.

out of the ring-plane and therefore how far the π-systems are from nearest neighbors in the stack. Controlling the assembly could yield low-dimensional molecular semiconductors provided that the stacking along the direction of the column involves strong $\pi-\pi$ overlap between molecules.[9] For these applications, it is important to understand how the solution phase electronic structure can be transferred to the substrate. ^{1}H NMR experiments that have proven useful in understanding the dynamics of other π-stacked systems in solution[10] are inconclusive here due to the absence of protons on the central aromatic ring.

In this work we utilize site-selective wavelength-dependent fluorescence spectroscopy——a valuable technique to understand the self-organization in solution for molecular systems such as proteins, peptides, and membrane-bound probes[11]——to determine whether **1** and **2** self-assemble into columnar structures in solution. Our approach is based on the different fluorescence response from individual molecules, which we will call "monomers," compared to molecules stacked to form columns, which we will refer to "aggregates" (see Figure 2b for the schematic drawing). The terms "fibers" or "aggregates" will be used interchangeably to refer to the 1D structures when visualized by microscopy. Furthermore, these fibers/aggregates form species with ground and excited electronic properties distinct from that of the monomer. We selectively excite the monomers or the aggregates to obtain information about the assembly processes in solution. The excited state of the aggregate is significantly longer lived than that from the isolated molecules and easily observed in time-resolved photoluminescence experiments. Aggregates for both **1** and **2** could be detected in methylene chloride solutions as low as 10^{-7} M. Spectroscopy and microscopy of films cast from solutions of **1** and **2** provide strong evidence that the structural integrity of the aggregates in solution is preserved during the transfer process onto the substrate.[12] Thus, we can use the solvent to control the film morphology. Further organization of these aggregates into films with higher order structures is determined by whether the surface is hydrophilic or hydrophobic.

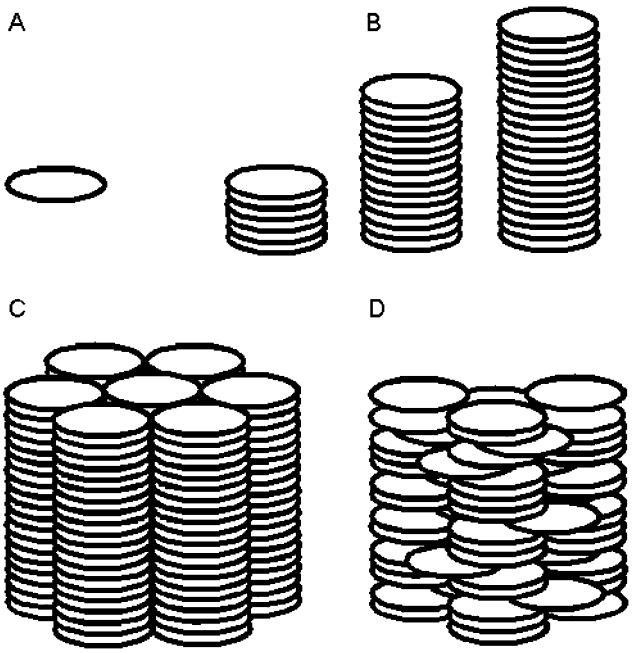

Figure 2. Schematic representation of possible molecular arrangements of compound **1**: (A) monomer; (B) aggregates/fibers of different sizes; (C) a bundle of aggregates/fibers; (D) a complex, ill-defined packing structure.

II. Experimental Section

The hexasubstituted aromatics **1** and **2** used here were synthesized according to the published procedures.[7] Solutions were made by stirring for several hours compounds **1** and **2** in either anhydrous or spectroscopic grade methylene chloride (Aldrich). For experiments on the solvent dependence, solutions of **1** and **2** were made in anhydrous methanol, methylene chloride, dodecane, and a mixture of methylene chloride and methanol (4:1, volume:volume) at the concentration of ca. 10^{-4} M. For the experiments on the concentration dependence, solutions of **1** and **2** were made in anhydrous methylene chloride at $\sim 10^{-4}$ M, and serial dilutions were used to prepare solutions at 10^{-5}, 10^{-6}, and 10^{-7} M. For the experiments on the temperature dependence, the photoluminescence (PL) and photoluminescence excitation (PLE) spectra (collected in 1 cm quartz cuvettes) of compound **1** and **2** (in CH_2Cl_2 and MeOH, 10^{-4} M) were collected at room temperature, then after the solution was cooled to 2 °C using an ice-bath for an hour and then after the solution again reached room temperature (24 °C). The same procedure was repeated except, this time the solution was cooled to −42 °C. Next, the solution was heated to 50 and 80 °C, and the PL and PLE spectra were collected.

In the morphology studies with the atomic force microscopy (AFM) and scanning electron microscopy (SEM), the solutions were either spin-coated onto the basal plane of freshly cleaved, highly oriented pyrolytic graphite (HOPG) or drop-cast onto clean silicon wafer with 100 nm of thermally grown SiO_2. The molecular films were dried in air for ~20 min before imaging. Similarly, the UV−vis and PL measurements were done at room temperature on quartz substrates cleaned just prior to the spin-coating the solutions. For each solution, the measurements were repeated on several films, and on each film

(8) For hydrogen bonds used to hold aromatic rings cofacially, see: (a) Matsunaga, Y.; Miyajima, N.; Nakayasu, Y.; Sakai, S.; Yonenaga, M. *Bull. Chem. Soc. Jpn.* **1988**, *61*, 207−210. (b) Yasuda, Y.; Iishi, E.; Inada, H.; Shirota, Y. *Chem. Lett.* **1996**, 575−576. (c) Palmans, A. R. A.; Vekemans, J. A. J. M.; Fischer, H.; Hikmet, R. A.; Meijer, E. W. *Chem. Eur. J.* **1997**, *3*, 300−307. (d) Lightfoot, M. P.; Mair, F. S.; Pritchard, R. G.; Warren, J. E. *Chem. Commun.* **1999**, 1945−1946. (e) Brunsveld, L.; Zhang, H.; Glasbeek, M.; Vekemans, J. A. J. M.; Meijer, E. W. *J. Am. Chem. Soc.* **2000**, *122*, 6175−6182. (f) Ranganathan, D.; Kurur, S.; Gilardi, R.; Karle, I. L. *Biopolymers* **2000**, *54*, 289−295. (g) van Gorp, J. J.; Vekemans, J. A. J. M.; Meijer, E. W. *Mol. Cryst. Liq. Cryst.* **2003**, *397*, 491−505. (h) Pucci, D.; Veber, M.; Malthete, J. *Liq. Cryst.* **1996**, *21*, 153−155. (i) Ungar, G.; Abramic, D.; Percec, V.; Heck, J. A. *Liq. Cryst.* **1996**, *21*, 73−86. (j) Malthete, J.; Levelut, A. M.; Liebert, L. *Adv. Mater.* **1992**, *4*, 37−41.

(9) Rochefort, A.; Martel, R.; Avouris, P. *Nano Lett.* **2002**, *2*, 877−880.

(10) (a) Martin, R. B. *Chem. Rev.* **1996**, *96*, 3043−3064. (b) Wang, W.; Li, L.-S.; Helms, G.; Zhou, H.-H.; Li, A. D. Q. *J. Am. Chem. Soc.* **2003**, *125*, 1120−1121. (c) Wang, W.; Han, J. J.; Wang, L.-Q.; Li, L.-S.; Shaw, W. J.; Li, A. D. Q. *Nano Lett.* **2003**, *3*, 455−458.

(11) (a) Chattopadhyay, A.; Mukherjee, S.; Raghuraman, H. *J. Phys. Chem. B* **2002**, *106*, 13002−13009. (b) Chattopadhyay, A.; Mukherjee, S. *Langmuir* **1999**, *15*, 2142−2148. (c) Rawat, S. S.; Mukherjee, S.; Chattopadhyay, A. *J. Phys. Chem. B* **1997**, *101*, 1922−1929.

(12) Similar to what was observed with for conjugated polymers, see: Nguyen, T.-Q.; Martini, I. B.; Liu, J.; Schwartz, B. J. *J. Phys. Chem. B* **2000**, *104*, 237−255.

multiple images were taken in different regions to ensure a good sampling of the film morphology and high reproducibility.

Topographic images of compounds **1** and **2** cast from different solvents were obtained using a Nanoscope IIIa/Bioscope Scanning Probe Microscopy from Digital Instruments. Etched silicon tips with a typical spring constant of 1−5 N/m and a resonant frequency of 50−80 kHz (NanoSensors) were used. The AFM images were collected in air under ambient conditions using the tapping mode. The PL and PLE spectra were measured on a Fluorolog-2 (Instrument S. A. & Co.) using a xenon lamp for the excitation source. The solution fluorescent lifetimes were measured using a commercially available time-correlated single photon counting instrument (Edinburgh Instrument, model FL900 CDT). The excitation source was a nanosecond flash lamp and the fwhm of the instrument response function was less than 0.7 ns. The fluorescence decays were collected at the magic angle of polarization. The lifetime data were deconvoluted from the instrumental response and fitted to single or double exponential equations.

III. Results and Discussion

From previous studies on both **1** and **2**, it has been elucidated that the main forces that guide the assembly are hydrogen bonding and $\pi-\pi$ interactions. The study below takes a closer look at this assembly process in solution as method to guide the formation of isolated nanostructures on surfaces. In these materials a balance must be met between the subunits affinity for itself and for its substrate. On one hand, when the stacking forces between molecules are great the assemblies grow too large to be effectively solvated and precipitate into ill-defined superstructures. On the other hand, if the association between the subunits is too slight, the $\pi-\pi$ overlap between conjugated cores will be diminish and interactions with the surface will dominate, resulting in a face-on orientation on the surface.[4] The steric bulk of the side chains on this crowded core is one of the determining factors of how well these molecules self-assemble.[7] Besides the side group and its interplay with the core size, the solvent is also a crucial factor in the self-assembly process. This process can be an entropy driven process when the solvent molecules are released upon the self-assembly formation,[13] but if the solvent has very strong interaction with the molecules, the aggregate cannot be formed. Below, we monitor the assembly of **1** and **2**, which have different groups on the alkynes flanking their amides (either hydrocarbon for **1** or phenyl for **2**), and probe how this assembly is crucially effected by the environment (solvent, temperature, and concentration). These solution-phase aggregates predetermine (both in terms of quality and quantity) the type of nanostructured morphology manifest in thin films.

A. Effects of the Side Groups and Evidence of Self-Assembly in Solution. Here we show that the self-assembly process exists in solution prior to the deposition of the supramolecular assembly on the surface. Figure 3 shows the normalized absorption and photoluminescence (PL) of **1** and **2** in methylene chloride. Several observations can be made from this simple comparison. First, for **2**, the substitution of central ring with the phenylethynyl groups at R″ substituent causes a red shifting of ca. 40 nm in the absorption and ca. 20 nm in the emission compared to **1** with an alkyl group substituting the alkyne on the central aromatic ring at the R″ position. The red shifting is due to the larger conjugated core of compound **2** compared to **1**. Second, for both compounds, the PL spectra

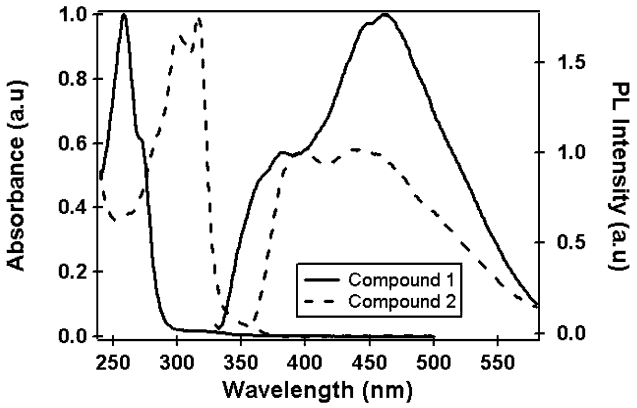

Figure 3. Normalized (at the monomer peak) absorption and PL spectra of **1** and **2** in methylene chloride (concentration = 10^{-5} M, λ (excitation) = 290 nm for **1** and 320 nm for **2**).

have a bifurcated peak structure. As explained below, one peak is from the monomers, and the other is from the aggregates (the red-shifted peaks). Third, the ratio of the monomer/aggregate peak of **2** is larger, meaning that the concentration of monomers in the solution is higher in **2** than in **1**. Last, while the monomer emission is similarly shifted compared to that of the absorption spectra, the aggregate emission from compound **2** is blue-shifted relative to that from the aggregate of **1**. One explanation for this blue shift in the aggregates with the larger aromatic core is that the freely rotating phenyl group on the ethynyl-substituents causes problems in the packing.

The emission spectra can be understood by considering the fact that the molecules **1** and **2** stack in solution into columnar aggregates. These supramolecular structures have been described previously[7] to form helical stacks with an intermolecular distance for the co-facially arranged aromatic rings to be within their van der Waals radii. In PL, the excited state of the monomers is localized on a single molecule, and the emission wavelength depends mostly on the size of the conjugated core. In contrast, the emission of the columnar structure is red-shifted relative to the monomer, because it has an excited state that is delocalized over several subunits/molecules within the stack. The delocalization of the excited state wave function across several molecules lowers the energy relative to the localized excited state of the monomer resulting in a red-shifted luminescence from the aggregate. Of course, if the aggregate has poor overlap between the molecular subunits, the excitation will be more localized and therefore at a wavelength closer to the monomer emission. Thus, the position of the emission peak provides a good characterization of the intermolecular interaction in the aggregates; i.e., aggregates with stronger interactions present emission spectra that are red shifted compared to weakly interacting aggregates.[14] The monomer peak at about 370−390 nm is clearly resolved from the broad structure in the emission at wavelengths between 400 and 600 nm, which originates from the aggregates. The broad emission spectrum of the aggregates suggests a wide distribution of sizes or the presence of different forms of aggregates. This point will be discussed further below.

Figure 4 shows the PLE (Figure 4a) and PL (Figure 4b) spectra of **1** in methylene chloride collected as the excitation and emission are moved to longer wavelengths. Because both **1** and **2** show similar results, only the results of **1** are presented

(13) Yau, S. T.; Petsev, D. N.; Thomas, B. R.; Vekilov, P. G. *J. Mol. Biol.* **2000**, *303*, 667−678.

(14) Shirai, K.; Matsuoka, M.; Fukunishi, K. *Dyes Pigm.* **1999**, *42*, 95−101.

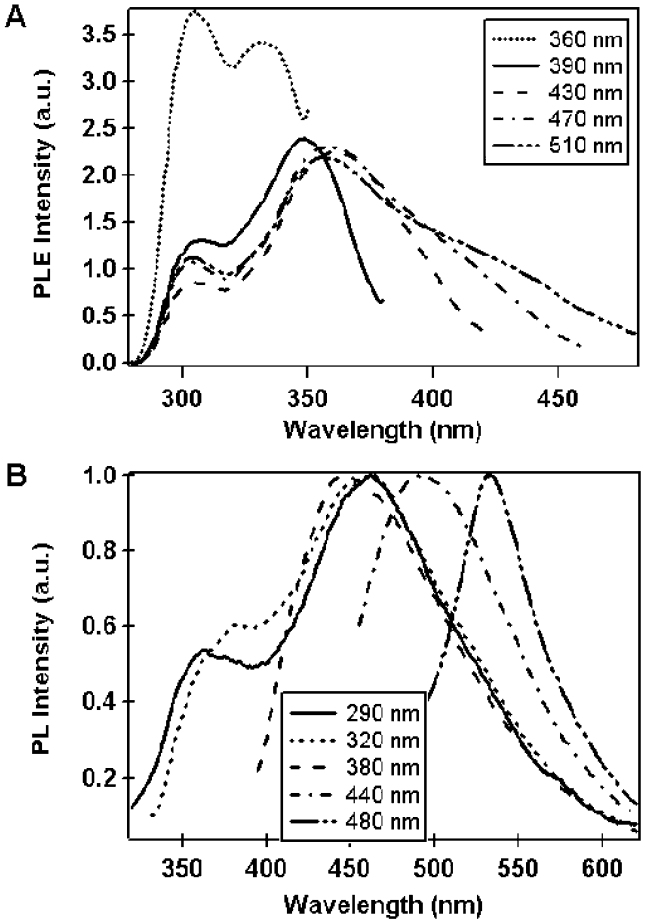

Figure 4. (A) PLE and (B) normalized PL spectra of compound **1** in methylene chloride collected at different emission and excitation wavelengths.

below. Similar PL spectra for **2** are shown in the Supporting Information. A large red shift is observed in both PLE and PL spectra as the emission and excitation wavelengths increase. Generally, this red shift is either due to the strong electronic interactions among the chromophores or to the motion of chromophores in a restricted condensed media such as in a very viscous solution, in a membrane or in a micelle.[10] For the experiments performed here, the solvents used, i.e., methylene chloride and methanol, have similar viscosity (0.413 vs 0.544 cP at 25 °C), while the viscosity of dodecane is three times larger (1.383 cP at 25 °C). However, there is no shift in the PL spectra for dodecane with increased excitation wavelength (see section B for the effect of solvent).[15] Therefore, we can rule out the contribution of the red-shifted PL due to the increase in the solution viscosity. In addition, there are many cofacially stacked π-systems that show red-shifted absorbance and emission upon aggregation.[16]

(15) *CRC Handbook of Chemistry and Physics*, 76th ed; CRC Press: Boca Raton, FL, 1995−1996; pp 6-245 and 6-249.

(16) (a) Sheu, E. Y.; Liang, K. S.; Chiang, L. Y. *J. Phys. (Paris)* **1989**, *50*, 1279−1295. (b) Braitbart, O.; Sasson, R.; Weinreb, A. *Mol. Cryst. Liq. Cryst.* **1988**, *159*, 233−242. (c) Markovitsi, D.; Germain, A.; Millie, P.; Lecuyer, P.; Gallos, L.; Argyrakis, P.; Bengs, H.; Ringsdorf, H. *J. Phys. Chem.* **1995**, *99*, 1005−1017. (d) Phillips, K. E. S.; Katz, T. J.; Jockusch, S.; Lovinger, A. J.; Turro, N. J. *J. Am. Chem. Soc.* **2001**, *123*, 11899−11907. (e) Nuckolls, C.; Katz, T. J.; Katz, G.; Collings, P. J.; Castellanos, L. *J. Am. Chem. Soc.* **1999**, *121*, 79−88. (f) Nuckolls, C.; Katz, T. J. *J. Am. Chem. Soc.* **1998**, *120*, 9541−9544. (g) Rohr, U.; Schilichting, P.; Bohm, A.; Gross, M.; Meerholz, K.; Brauchle, C.; Mullen, K. *Angew. Chem., Int. Ed.* **1998**, *37*, 1434−1437. (h) Reference 10b,c.

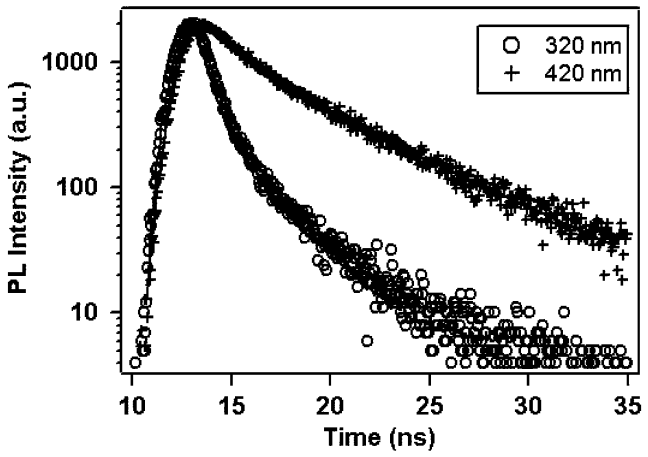

Figure 5. The fluorescence decays of compound **1** in methanol: the monomer was excited at 320 nm, and its emission was monitored at 380 nm (opened circles); the aggregates were excited at 420 nm, and their emission were monitored at 480 nm (crosses); the fit to each curve is shown as solid line.

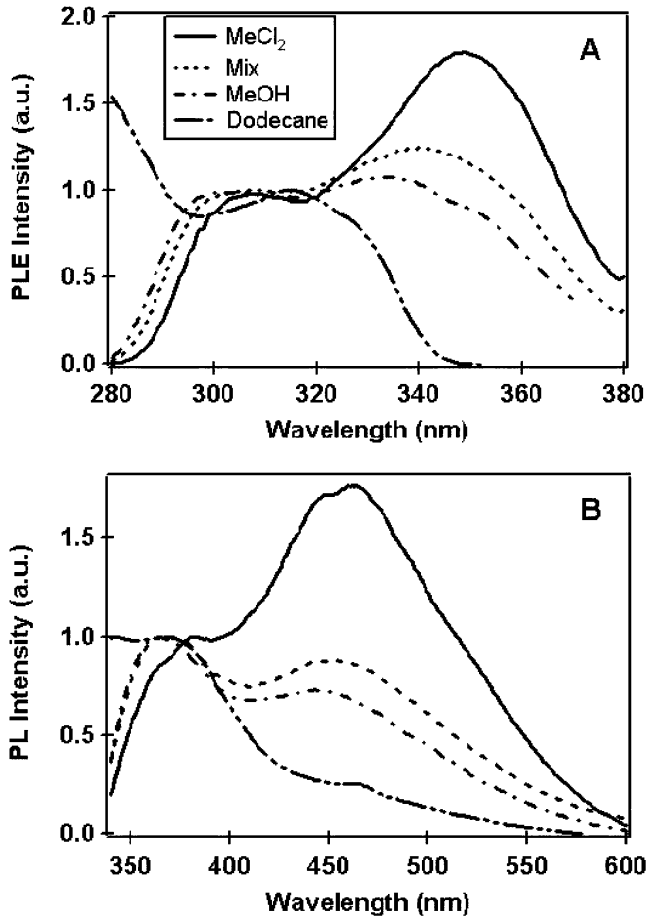

Figure 6. (A) PLE and (B) PL spectra of compound **1** in different solvents: methylene chloride ($MeCl_2$, solid curve), mixture of methylene chloride and methanol (4:1 by volume) (mix, dashed curve), methanol (MeOH, dashed−dotted curve), and dodecane (short-long-short dashed curves). They are normalized at the monomer peak (310 nm for PLE and 360 nm for PL). The excitation was at 320 nm, and the emission was collected at 360 nm.

PLE spectroscopy has no interfering background, so it is very sensitive at low concentration. This is why the red-shifted absorption/aggregate bands in Figure 4a at low concentration are observed only in the PLE spectra and not in the UV−visible

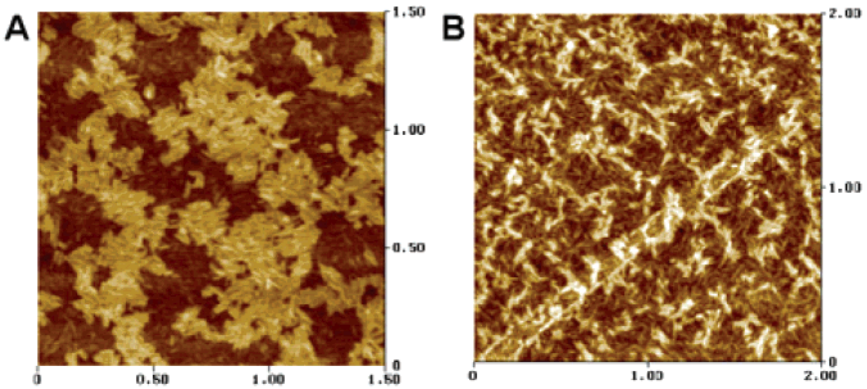

Figure 7. Topographic images from methylene chloride spin-cast on graphite for (A) compound **1** and (B) compound **2**.

absorption spectra. As seen in Figure 4, the emission from the aggregates can be enhanced by preferentially exciting toward longer wavelengths (400−500 nm) of PLE band maxima. Figure 4b plots the normalized PL spectra of **1** excited at 290 nm (the peak of monomer exciton absorption) and at longer wavelength, 360−480 nm (aggregate band). The fluorescence spectra show that the aggregate emission shifts continuously to the red with the excitation wavelength. This can be explained in terms of a wide distribution in the aggregate length and number. From the PL spectra, it is difficult to estimate the size or number of the aggregates because their absorption spectra consist of a superposition of states with transition energies varying continuously. Moreover, their absorption cross-sections are unknown. Nevertheless, the results presented here provide direct evidence for aggregate formation in solution. The aggregate and its size can be visualized and estimated from the AFM and SEM images in section C below.

To further characterize the aggregates in solution, we measure the lifetimes of the excited states at different excitation and emission wavelengths. Because of the difference in the excited states between the aggregates and the monomers, the lifetimes are expected to be quite different. Our ability to excite selectively one or the other allows us to test this idea; i.e., the aggregate excited state would have a longer lifetime due to the delocalization through several π-stacked monomer units. With the correct choice of excitation and emission wavelengths, the excited-state dynamics of the monomer and the aggregate are measured independently. From the PLE results in Figure 4, we select the excitation for the aggregate in the red portion of the main absorption band ($\geq$400 nm), while the monomer is obtained with excitation in the blue portion ($\leq$350 nm). Figure 5 shows the fluorescent decay dynamics of compound **1** in methanol. Methanol was used because there was a substantial amount of the monomer present. In this experiment, the monomer is excited at 320 nm, and the emission is collected at 380 nm. Since the aggregate emits much further to the red, we set the excitation to 420 nm, and the emission was collected at 480 nm. The decay curve at 320 nm excitation in Figure 5 was fitted to a single exponential with the lifetime of 1.72 ns—presumably dominated by the monomer lifetime. The decay at 420 nm excitation, however, fits to two lifetimes, one at 5.72 ns and one at 1.46 ns. The longer lifetime, 5.72 ns, is clearly the decay dynamic of the aggregates. The difference in the shorter lifetimes (1.72 ns versus 1.46 ns) is likely due to the error introduced by the assumption that the decay curve is fit with only two distinct lifetimes when in reality the decay is more complicated and probably involves several type of aggregates with different lengths and therefore different lifetimes. In methylene chloride **1** also shows two distinct lifetimes—one at 7.08 ns and the other at 1.70 ns.

B. Effects of the Solvents on the Aggregation of Compound 1 in Solution. In this section, we examine the effects of solvents on the molecular packing of molecule **1**. The aggregation process is a result of more favorable molecule-molecule interactions over molecule−solvent interactions.[17] If the interaction between solutes and solvent molecules is stronger than molecule-molecule and solvent−solvent interactions, there would be very few aggregates in the solution and mostly monomers. On the contrary, if the molecule−solvent interaction is weak, there would be very few monomers present in solution. Figure 6 shows the PLE and PL spectra of **1** (normalized at the monomer emission peak) in methylene chloride, methanol, a mixture of methylene chloride and methanol (4:1 by volume, referred to as "mix" in Figures 6 and 9), and in dodecane at the same concentration (10^{-4} M). The aggregate absorption and emission peak positions and intensities are used to estimate their numbers and sizes. From Figure 6, the aggregate peak is red-shifted and increases in intensity as it goes from dodecane, pure methanol, mixed solvent, to methylene chloride. This implies that there is a higher degree of aggregation in pure methylene chloride than in the other solvents tested. In methanol, however, the number of monomers increases due to the additional competition for the hydrogen bonds between the solvent and the molecules.

As we go from methylene chloride to mixed solvents and then to pure methanol, the monomer emission increases smoothly with the methanol concentration probably due to the competition for the hydrogen bonding with the solvent. This effect is clearly seen from the spectra of the mixed solvent. However, there is still a measurable number of aggregates in these two solutions, indicating that hydrogen bonding is not the only force that holds the molecules together in the aggregates. For example, $\pi-\pi$ interactions and solvophobic effects between the aromatic cores can also play an important role in holding the molecules together. As discussed below, methanol takes an active part in the formation of a new complex aggregate structure for **1**.

Surprisingly, the aggregate emission in dodecane is very weak and most, if not all, of the PL emission is from the monomer. This effect is likely due to the strong solvophobic interactions between the solvent and the long alkyl chains attached to the

(17) Attard, P. *Mol. Phys.* **1996**, *89*, 691−709.

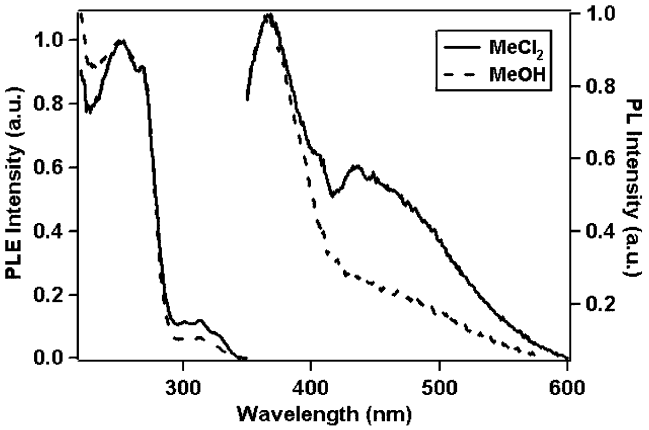

Figure 8. PLE and PL of compound **1** in methylene chloride ($MeCl_2$, solid curve) and in methanol (MeOH, dashed curve) spin-cast on quartz substrates. The spectra are normalized at the monomer peak. The PLE spectra were collected at 360 nm and the PL spectra were excited at 320 nm.

monomer. The solvent stabilizes the monomer in the solution and therefore interferes with the packing process. This result is unexpected and coupled with the results from the studies with methanol indicate that not only hydrogen bonds but also solvophobic forces from the side chains and the core facilitate the assembly.

C. Effects of the Solvent and the Substrate on the Film Morphology. As we spin cast the solutions of **1** and **2** in methylene chloride onto graphite ($\sim 10^{-4}$ M), high-aspect ratio aggregates can be seen in the film morphology shown in 7. The topographic images of **1** (Figure 7a) and **2** (Figure 7b) are of short fibers packed closely together in random directions. The fibers of **1** are straight and packed closely to from ordered sheets/layers. However, this is not the case for **2**. The fibers of compound **2** have the tendency to tangle together and form poorly defined layers. We speculate that this disorder is related to the freely rotating phenyl groups on the triple bonds that introduce steric interaction in the assembled structure.

The emission spectra of these fibrous films can be correlated with the type of solvent that is used for the casting. The important point is *not* that the exact morphology of a film is present in solution, but rather that the size and number of the underlying aggregates in a thin film is a consequence of concentration and the type of solvent used. Figure 8 displays the PLE and PL of compound **1** spin cast from methylene chloride and methanol solutions. When the films are spin-cast from methylene chloride, the aggregate absorption and emission bands are relatively high in intensity (vide infra). For methanol the long wavelength aggregate emission is substantially attenuated (Figure 8) implying that the delocalized aggregates are less in films from methanol. Again, this is qualitatively the same behavior observed in solution.

Figure 9 presents the AFM topology of films made with compound **1** ($\sim 10^{-4}$ M) on graphite obtained by spin casting from methylene chloride, methanol, a mixture of methylene chloride/methanol, and dodecane at room temperature. The film in Figure 9a from methylene chloride is composed of short fibers arranged in a multilayered film ordered over small domains of

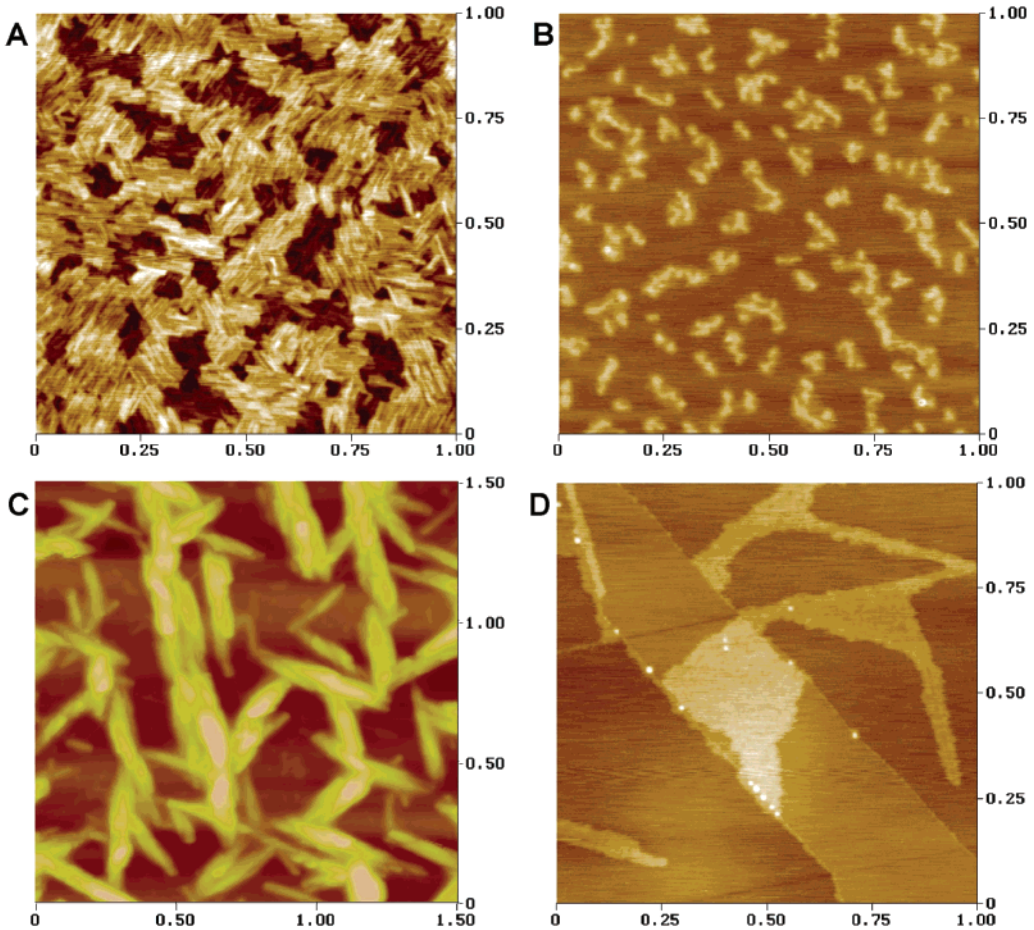

Figure 9. Topographic images of compound **1** in (A) methylene chloride, (B) mix, (C) methanol, and (D) dodecane spin-cast on graphite.

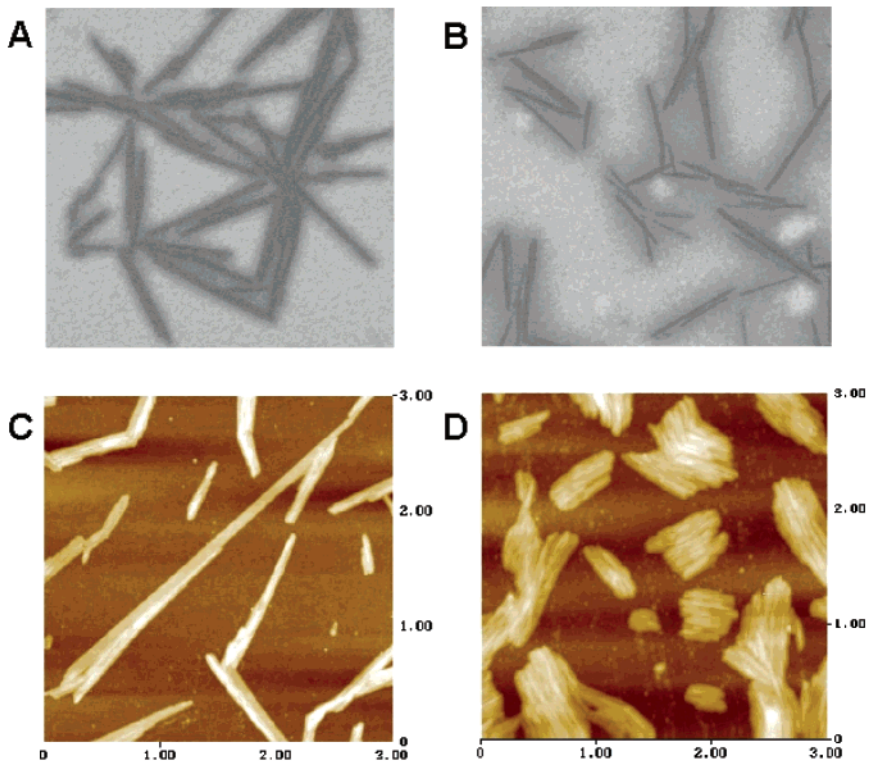

Figure 10. (A, B) SEM (2 μm × 2 μm) and (C, D) AFM images of compound **1** in methylene chloride drop-cast (SEM) and spin-cast (AFM) on Si/SiO_2.

about 0.1 μm × 0.1 μm. In the same conditions, the film cast obtained with the mixed solvent (methylene chloride/methanol) in Figure 9b has a much lower number of fibers. Thus, the AFM results agree very well with our interpretation of the PL data for both solutions. The electronic structure of the films evidenced by the long wavelength emission survives the casting process.

The films obtained from the methanol solution contain large, tangled bundles with complex packing structures (Figure 9c). For this solution, the PL spectra show a lower concentration of aggregates relative to the monomer, probably resulting from the strong competition for hydrogen bonding with the solvent. This competitive action prevents the formation of fibers with isolated columns (with a diameter of 1∼1.9 nm)[4] in favor of larger physical aggregates (with the diameter of ca. 30−50 nm) that have no influence on the optical properties of **1** in methanol. Presumably, the aggregate size in this bundle is smaller and there are fewer numbers of aggregates in methanol-cast film than for methylene chloride-cast film. This is in agreement with the blue shifted peaks of the aggregate emission in the PL emission when compared to the fibers emission observed in methylene chloride. These observations are consistent with poor molecular packing of units that interact weakly with each other. Thus, it is likely that the solvent participates in this packing structure by competing for hydrogen bonding.

The case of the dodecane solution is rather simple. It forms a film on graphite (see Figure 9d) with only a few aggregates/fibers. The material deposited is mostly embedded in a featureless layer. In dodecane, although hydrogen bonds can be formed, this system does not favor the assembly and yields poor results. This is again consistent with the PL results described above.

The interaction between the molecule and the surface is important for guiding the patterns formed by the film, such as the orientation of the fibers and their size or number on the surface. For example, compound **1** deposited on graphite at low concentration (∼10^{-6} M) gives fibers that are spread out to form a monolayer on graphite, due to the strong van der Waals interaction between graphite and the molecules. The fibers are straight, packed parallel and in registry with the graphite lattice at either 60° or 120° angles. On Si/SiO_2 (see Figure 10), the fibers have the tendency to form bundles (7−50 nm in diameter) and orient randomly. This is a result of a less favorable interaction between this hydrophilic substrate and the hydrophobic aggregates. Thus, the fibers bundle up together to minimize the interactions with the surface and optimize the van der Waals interaction among the fibers. Also, from the AFM and SEM images, we are able to estimate the size of the aggregates/fibers. Figure 10 shows representative AFM and SEM images of compound **1** in methylene chloride drop-cast (SEM) and spin-cast (AFM) onto Si/SiO_2 substrate. Examining various regions within the same film reveals a wide range of the fiber length from 200 to 4 μm. If the distance between monomers is estimated to be ca. 0.35 nm, a 1 μm long fiber is comprised of a few thousand molecules. It is unlikely that a single fiber that long can be stabilized in solution. They are probably forming bundles in solution through van der Waals interactions. In films, the fiber−fiber and fiber−surface interactions help stabilize longer aggregate structures.

D. Effects of Concentration and Temperature. To understand how temperature influences the aggregation of **1**, we collected the PL of **1** in methylene chloride at room temperature, 50, 80,−2, and −40 °C. We observed no apparent change in the PL intensity or the emission peak in the PLE and PL spectra as the solution was cooled. At higher temperatures (50 and 80 °C), the PL intensity decreases slightly when the monomer band is excited, probably, due to the monomer PL quantum yield is

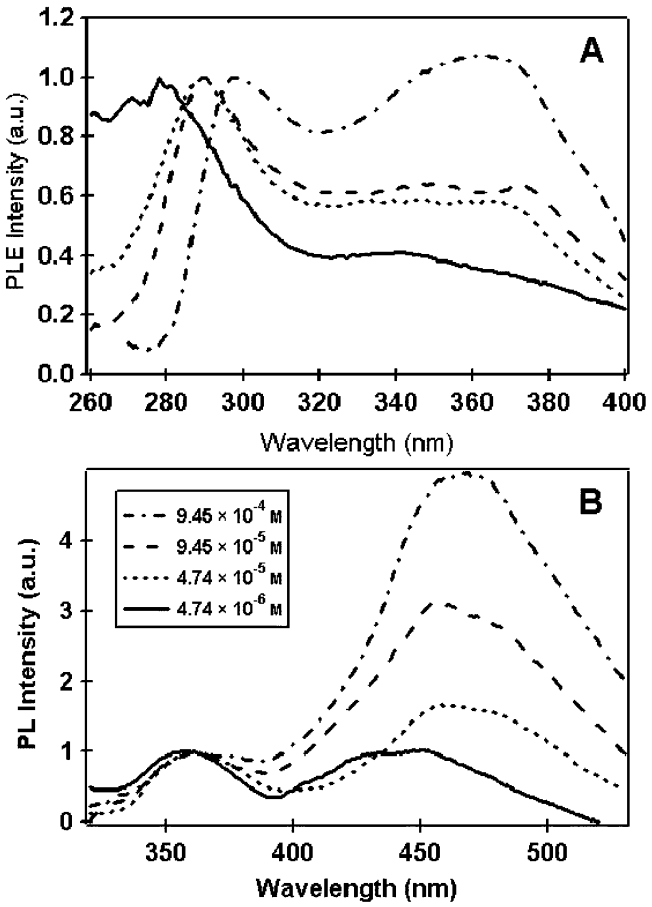

Figure 11. (A) PLE and (B) PL spectra of compound **1** in methylene chloride at different concentrations: 9.45×10^{-4} M (dot−dashed curve), 9.45×10^{-5} M (dashed curve), 4.74×10^{-5} M (dot curve), and 4.74×10^{-6} M (solid curve). The PLE (collected at 420 nm) and PL (excited at 270 nm) spectra are normalized at the monomer peak.

lower at this temperature. There is no apparent change in either the PL intensity or the emission peak maximum as we excite the aggregate band at higher temperatures. Films cast from this solution show both fibers and some monomers. Heating these films does not change the orientation of the molecules with respect to the surface (face-on or edge-on orientations) or the number of the monomers/aggregates. We observe only phase segregation between the monomers and the aggregates (data not shown).

Next, we investigate the effects of concentration on the way the molecules pack in solution and on the film morphology. Figure 11 presents the PLE and PL spectra (normalized at the monomer emission peak) of **1** in methylene chloride at different concentrations, $\sim 10^{-4}$, $\sim 10^{-5}$, and $\sim 10^{-6}$ M. As the concentration increases, a new band appears in the red part of the PLE spectrum. This peak is at about 360 nm, and it is related to the fibrous structures seen with the AFM (Figures 9 and 12). In addition, the number of fibers/aggregates increases with concentration, as seen in the enhancement of the red-shifted emission (aggregate emission at 450 nm). The PL spectra are also red-shifted with an increase in concentration, which is a signature of the formation of aggregates in solution. This can also be seen in the film morphology as shown in Figure 12. At high concentration, the fibers are short and pack closely together. They also form a multilayered film on the graphite substrate (Figure 12a and Figure 9a). As the concentration of the solution decreases, the fiber length increases and creates isolated stacks of fibers, oriented according to the graphite lattice (Figure 12b). This can be explained using basic concepts of crystal growth, but in this case, it is a one-dimensional growth process. There are several factors that influence the numbers of fibers formed and their length. These are the nucleation sites, the nucleation rate, and the growth rate. Generally, the nucleation sites, which determines the number of fibers formed, increase with the concentration, and this is the same for the nucleation rate.[18,19] The growth rate is controlled by the diffusion process, and hence, at higher concentration or higher temperature, the probability that the molecules encounter a nucleation site increases.[19,20] Consequently, the monomer depletion rate is much higher for concentrated solution than for dilute solution. Thus, there are more fibers in concentrated solution, but they are much shorter compared to the low concentration. Therefore, concentration can be used to control the length and number of the fibers formed.

IV. Conclusions

In summary, we have shown that intermolecular interactions such as hydrogen bonds and $\pi-\pi$ interactions guide the aggregate formation in solution. These interactions can be used to fabricate 1D organic molecular wires. Various functional side-groups can be used to tune the interaction among the subunits within the columnar stack and the orientation of molecules on a surface. We found that the columnar stacks/aggregates are

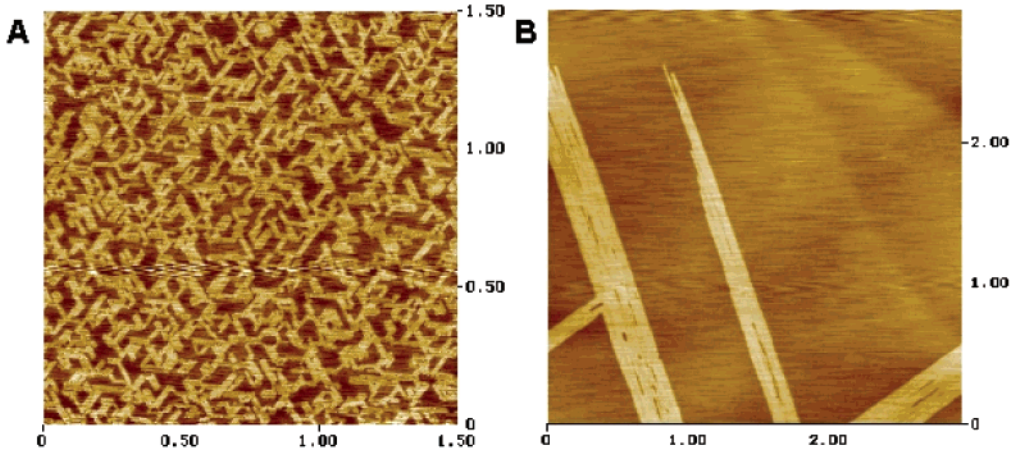

Figure 12. AFM images of compound **1** in methylene chloride at different concentration spin-cast on graphite: (A) 9.45×10^{-5} and (B) 9.45×10^{-6} M.

formed in solution prior to casting on the substrate, as is evident in the red-shifted absorption and emission and the longer-lived fluorescence for the aggregate compared to the monomer. We found that the degree of aggregation is solvent- and concentration-dependent. The degree of aggregation increases with the concentration and is highest in methylene chloride and lowest in dodecane. These results are interpreted with the interplay of the interactions involved—molecule−molecule versus solvent−molecule. Our results suggest that the solution history of the self-assembly is retained through the casting process. Thus, the processing conditions such as solvent, concentration, and type of substrate used provide control on the size, orientation and number of the aggregates formed. Finally, we proposed that the self-assembly of hexasubstituted aromatics such as **1** and **2** into columnar structures can be converted into different aggregate structures using a solvent that offers competitive channels for hydrogen bonding. By the proper tuning of the chemical functionality, these columnar structures can be used as model systems for investigating the charge transport in 1D semiconducting organic nanostructures.

(18) Galkin, O.; Vekilov, P. G. *J. Am. Chem. Soc.* **2000**, *122*, 156−163.
(19) Lin, J.; Zhu, J.; Zhou, D. *Eur. Polym. J.* **1999**, *36*, 309−314.
(20) Petsev, D. N.; Chen, K.; Gliko, O.; Vekilov, P. G. *Proc. Natl. Acad. Sci. U.S.A.* **2003**, *100*, 792−796.

Acknowledgment. We thank Professor Nicholas Turro and Dr. Steffen Jockusch for the use of the fluorometer and time-correlated single photon-counting instrument. We thank Prof. Fotios Papadimitrakopoulos (University of Connecticut) for stimulating discussion. We acknowledge primary financial support from the Chemical Sciences, Geosciences and Biosciences Division, Office of Basic Energy Sciences, US D.O.E. (#DE-FG02-01ER15264), US National Science Foundation CAREER award (#DMR-02-37860), and the Nanoscale Science and Engineering Initiative of the National Science Foundation under NSF Award Number CHE-0117752 and by the New York State Office of Science, Technology, and Academic Research (NYSTAR). C.N. thanks the Beckman Young Investigator Program (2002), the NYSTAR J. D. Watson Investigator Program (2003), The American Chemical Society PRF type G (#39263-G7), and the Dupont Young Investigator Program (2002) for support. M.L.B. thanks the ACS Division of Organic Chemistry for a graduate fellowship sponsored by Bristol-Myers Squibb.

Supporting Information Available: PL spectra of **2** at different wavelengths (PDF). This material is available free of charge via the Internet at http://pubs.acs.org.

JA031600B